4 IFITM3 restricts the morbidity and mortality associated with influenza.

4.1 Introduction

The IFITM family of proteins represents an important intrinsic and innate block to viral infection. Initially identified as playing a role in development and germ cell homing (Tanaka *et al.* 2004; Tanaka *et al.* 2005), IFITM3 has subsequently been shown to block an increasing number of viruses *in vitro*, which currently includes influenza A and B viruses (IAV and IBV), flaviviruses such as West Nile virus (WNV) and dengue virus, and Ebola virus, amongst others (Brass *et al.* 2009; Jiang *et al.* 2010; Weidner *et al.* 2010; Feeley *et al.* 2011; Huang *et al.* 2011; Schoggins *et al.* 2011; Anafu *et al.* 2013; Mudhasani *et al.* 2013; Wilkins *et al.* 2013).

As described briefly in section 1.4.1, the IFITM family consists of multiple members across various species. Interestingly, it appears as though the family has also diverged so that individual members are more capable of restricting certain viruses than others, with IFITM1 shown to have higher restrictive capacity against the filoviruses (Huang *et al.* 2011), whilst IFITM3 has been shown to be more capable of restricting influenza viruses (Brass *et al.* 2009). IFITM3 is thought to be associated with late endosomal membranes, where it effectively blocks the release of viruses into the cytosol (Weidner *et al.* 2010; Feeley *et al.* 2011). However, as discussed in section 1.4.1, the exact biochemical function of IFITM3 has yet to be elucidated, although it does appear to be playing a role in membrane fusion, potentially through moderation of cholesterol homeostasis (Figure 1.16) (Amini-Bavil-Olyaee *et al.* 2013; John *et al.* 2013). Additionally, a reported association with vacuolar ATPase complex suggests a role in mediation of endosomal pH and clathrin-mediated phagocytosis (Wee *et al.* 2012).

Analysis of the amino acid structure of IFITM3 and its post-translational modifications through palmitoylation and ubiquitination has aided in furthering our understanding of its mode of action (Yount *et al.* 2012; John *et al.* 2013). Systematic, non-biased alanine scanning of IFITM3 has shown that the majority of the anti-influenza restrictive capacity is encoded in the protein's N-terminal residues (Figure 3.1) (John *et al.* 2013). Further to this, research has shown that the key IFITM3 domain determining its ability to restrict viruses resides within the N-terminal 20 amino

acids (Weidner *et al.* 2010). Together, these studies would suggest that the tyrosine residue at position 20 (Y20) is a functionally critical amino acid.

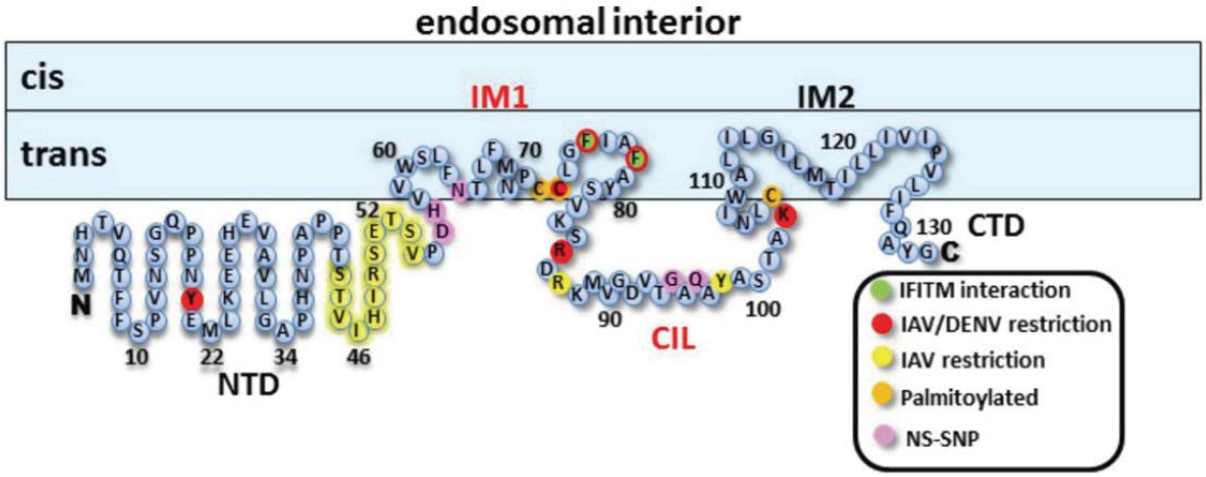

Figure 4.1: Analysis of each IFITM3 amino acid's influence on antiviral restriction of influenza and dengue viruses. Alanine-scanning mutagenesis was used to examine the individual amino acid's function on IFITM3-mediated restriction. The sites that most influenced the properties of IFITM3 are shown and explained in the legend, with NS-SNP indicating SNPs that occur in both IFITM2 and IFITM3. NTD: N-terminal domain; IM1: intra-membrane region 1; CIL: conserved intracellular loop; IM2: intra-membrane region 2; CTD: C-terminal domain. IM1 and CIL are shown in red to indicate that they comprise the two components of the CD225 domain. From (John *et al.* 2013)

The IFITM family has been implicated in multiple processes in addition to the immune system, such as primordial germ cell homing and cancer (Tanaka *et al.* 2005; Andreu *et al.* 2006). To investigate the effects of the IFITM family on primordial germ cell homing and embryonic development, Lange and colleagues (2008) generated a knockout mouse with an ablation of the entire *Ifitm* family locus to create an *Ifitm*^{del} mouse. Surprisingly, the mouse developed normally and was phenotypically similar to wild type littermates. In addition to this, they generated a targeted knockout of Ifitm3 to examine whether there were any gradient-dependent effects stemming from the loss of a single family member; this mouse line also showed no obvious phenotypic effect (Lange *et al.* 2008). The Ifitm3 knockout mouse (*Ifitm3*$^{-/-}$) was generated through the insertion of an EGFP locus into exon 1 of the coding sequence; thus generating EGFP instead of Ifitm3 upon stimulation (Figure 4.2). This mouse was used for the duration of the study to test for other phenotypic effects induced by pathogens.

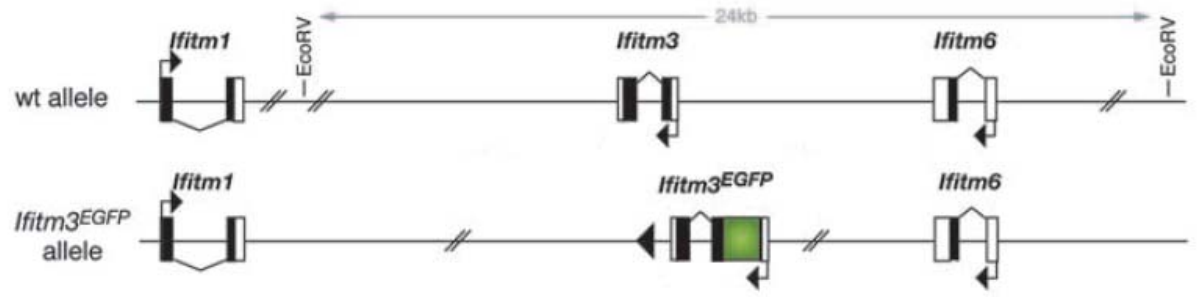

Figure 4.2: Schematic of the targeted ablation of the *Ifitm3* locus in *Ifitm3*$^{-/-}$ mice. The insertion of EGFP into exon 1 of the *Ifitm3* locus generated an Ifitm3-null mutant mouse. The *Ifitm3*^{EGFP} mouse will be referred to *Ifitm3*$^{-/-}$ for the remainder of the discourse. From (Lange *et al.* 2008)

Although humans do not carry an ablation of their *IFITM3* allele, multiple SNPs are reported across the length of the coding transcript (Figure 4.3). Currently, 13 non-synonymous, 13 synonymous, one in-frame stop and one splice site acceptor-altering SNPs have been reported in the *IFITM3* sequence, which could putatively have a dramatic effect on the activity or the expression pattern of the protein.

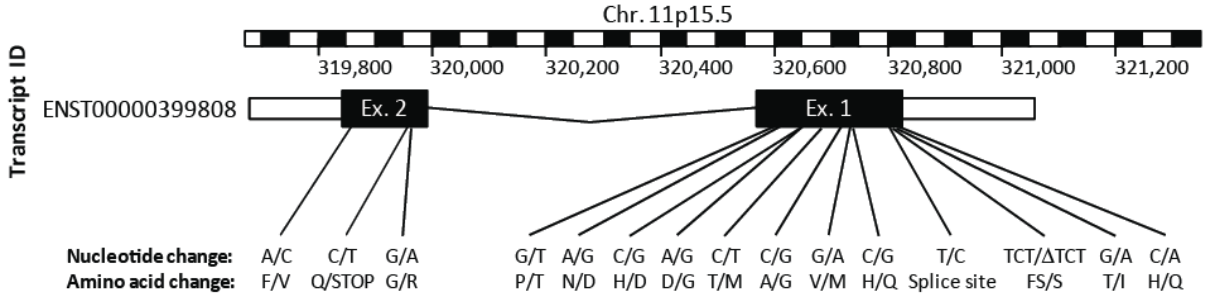

Figure 4.3: Single nucleotide polymorphisms of the *IFITM3* exons. All reported non-synonymous SNPs recorded in Ensembl are listed; noting the nucleotide change and its subsequent effects on the amino acid sequence.

The aim of the current study was to characterise the *Ifitm3*$^{-/-}$ mouse in terms of its susceptibility to influenza infection and for the first time, assess the role of Ifitm3 under virus challenge *in vivo*. Furthermore, a subset of individuals that were hospitalised during the H1N1 pandemic in 2009-2011, and had DNA samples taken as part of the Mechanisms of Severe Acute Influenza Consortium (MOSAIC) and Genetics of Influenza Susceptibility in Scotland (GenISIS) consortia, were analysed. In collaboration with Sarah Smith, we sought to sequence their IFITM3

loci and look for any discrepancies in the prevalence of SNPs within their alleles. Ultimately, the aim of the study was to move from cell lines to a model organism and translate those findings to humans.

4.2 Results

4.2.1 The impact of the loss of Ifitm3 on susceptibility to influenza virus infection in cell lines

To investigate the impact of the loss of Ifitm3 in mouse cells, RNAi studies were conducted in a murine alveolar epithelium cell lines (LA-4). Cells were transfected in duplex with either a scrambled siRNA or one specific to Ifitm3 and were subsequently infected with WSN/33 influenza virus at an MOI of 0.1 PFU/cell for 18 hours.

As shown in Figure 4.4, the targeted knockdown of Ifitm3 in the epithelial cell line resulted in significant increase in the levels of viral infection, with 12.6% of cells becoming infected, as opposed to 4.2% of cells when scrambled siRNA was used ($p = 0.001$).

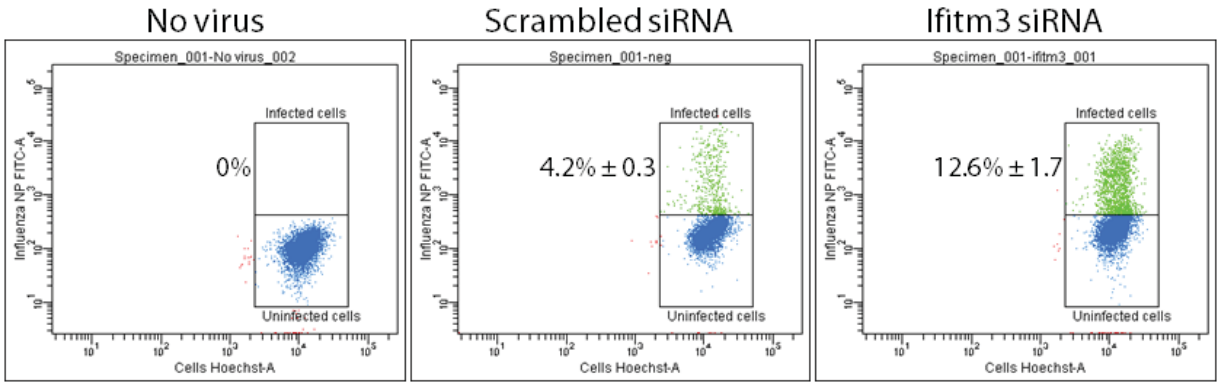

Figure 4.4: The impact of Ifitm3 knockdown in murine LA-4 cells. LA-4 cells were treated with either scrambled siRNA or siRNA specific to Ifitm3 and incubated for 48 hours. Cells were subsequently infected with WSN/33 influenza at an MOI of 0.1 PFU/cell for 18 hours and analysed for the expression of influenza NP (FITC) by flow cytometry. Figures indicate the mean ± SD of three biological replicates.

MEFs were also generated from wild type and *Ifitm3*$^{-/-}$ mice. Additionally, knock-in MEF lines were also created by the introduction of plasmids containing full length *Ifitm3* coding sequences into *Ifitm3*$^{-/-}$ cells to restore wild type expression. Cells were treated with IFNα or IFNγ for 24

hours and were challenged with either A/X-31 or PR/8 influenza at an MOI of 0.4 PFU/cell for 12 hours before being assayed for relative influenza protein expression.

As shown in Figure 4.5a, *Ifitm3*$^{-/-}$ MEFs were significantly more susceptible to influenza virus infection ($p < 0.0001$), regardless of whether they were pre-treated with IFN or not. The reintroduction of *Ifitm3* into *Ifitm3*$^{-/-}$ cells was also shown to return infectivity levels to comparable levels as the wild type cells (Figure 4.5b). The successful reintroduction of Ifitm3 was confirmed by Western Blot (Figure 4.5c).

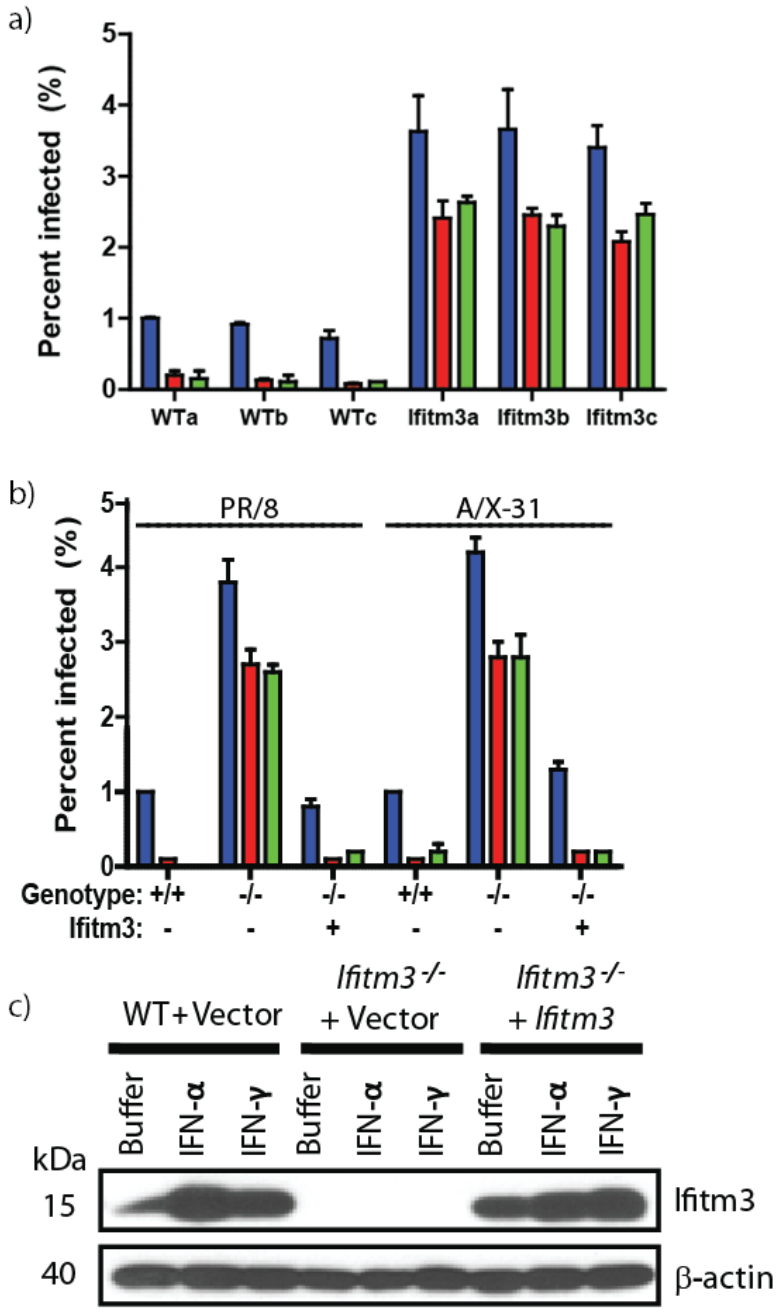

Figure 4.5: Infection levels of murine embryonic fibroblasts (MEFs) with and without the presence of Ifitm3 after influenza A challenge. MEFs from three different embryos from wt and *Ifitm3*$^{-/-}$ mice, denoted a-c, were challenged with PR/8 influenza virus following IFN treatment (a). Three lines of MEFs were generated: +/+, which are from wt mice, -/-, which are from *Ifitm3*$^{-/-}$ mice, and -/- with the reintroduction of Ifitm3 expression (b); "Ifitm3: -" indicates no plasmid was present, "Ifitm3: +" indicates presence of Ifitm3 plasmid. Similarly, these MEFs were challenged with either X-31 or PR/8 influenza virus. Transduction of *Ifitm3* into *Ifitm3*$^{-/-}$ was confirmed by Western blot (c). Results show means ± SD (n < 3). Blue bars: treated with buffer (control); red bars: IFNα treated; green bars IFNγ treated.

4.2.2 Confirmation of mouse genotype

Prior to further experimentation, mouse genotype and levels of Ifitm3 expression in the respiratory tissues were confirmed in wild type and *Ifitm3*$^{-/-}$ mice. PCR analysis of the locus revealed that the mice were assigned to breeding colonies correctly, with wild type mice possessing the full length *Ifitm3* coding sequence, whilst *Ifitm3*$^{-/-}$ mice possessed the *Ifitm3*$^{-/-}$ allele and insertion of EGFP, in accordance with the original publication (Figure 4.6a) (Lange *et al.* 2008). This genotype was confirmed by Western blot to assess for expression of Ifitm3 (Figure 4.6b).

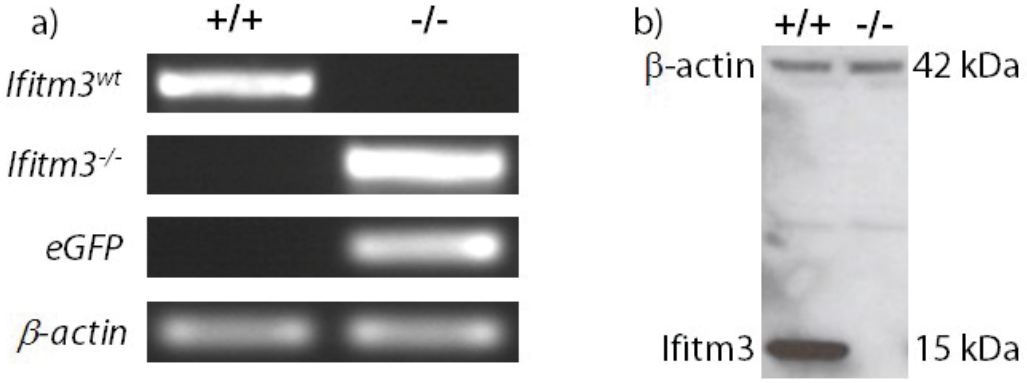

Figure 4.6: Confirmation of the loss of *Ifitm3* expression in *Ifitm3*$^{-/-}$ mice. DNA was extracted from lung tissue and analysed by PCR for the presence of full length (*Ifitm3*^{wt}) and ablated (*Ifitm3*$^{-/-}$) sequences, as well as the presence of *eGFP* which is inserted in the *Ifitm3* sequence in *Ifitm3*$^{-/-}$ mice (a). Protein was also extracted from lung homogenate and assayed by Western blot for the presence or absence of Ifitm3 (b). In both cases, β-actin was used as an endogenous loading control.

4.2.3 Influenza challenge of *Ifitm3*$^{-/-}$ mice

Mice were infected intra-nasally with 50µl of sterile PBS containing either A/X-31 (10^4 PFU), A/England/195/09 (200 PFU), wild type or delNS1 A/PR/8/33 (50-10^3 PFU) and monitored over the course of infection for clinical symptoms associated with severe illness (weight loss, piloerection, reduced motility etc.). Individuals were either culled at pre-determined time points or allowed to progress to monitor the overall weight loss profile. Mice that lost >25% of their original body weight were killed in accordance with UK Home Office regulations.

4.2.3.1 Weight loss and survival

All pathogenic viruses (X-31, England/195, PR/8) showed a similar statistically significant trend when comparing wild type to *Ifitm3*$^{-/-}$ mice, wherein *Ifitm3*$^{-/-}$ mice showed an accelerated weight loss and increased morbidity when compared to their wild type littermate controls (Figure 4.7). PR/8 was found to be highly pathogenic at the lowest accurately achievable dose (50 PFU in 50µl) and as such it was not possible to titrate the virus down any further in order to achieve wild type mouse survival. However, a statistically significant trend was still evident on days 4-6 post-infection, with the *Ifitm3*$^{-/-}$ showing significantly greater weight loss.

Infection with PR/8 delNS1 virus was conducted to assess whether *Ifitm3*$^{-/-}$ mice were IFN-competent and were capable of mounting an IFN response (Garcia-Sastre *et al.* 1998). The loss of the host-antagonist protein, NS1, results in an attenuated infection wherein the host mounts an unopposed IFN response to eliminate the virus. Infection with this virus resulted in no weight loss or morbidity differences between the wild type and *Ifitm3*$^{-/-}$ mice.

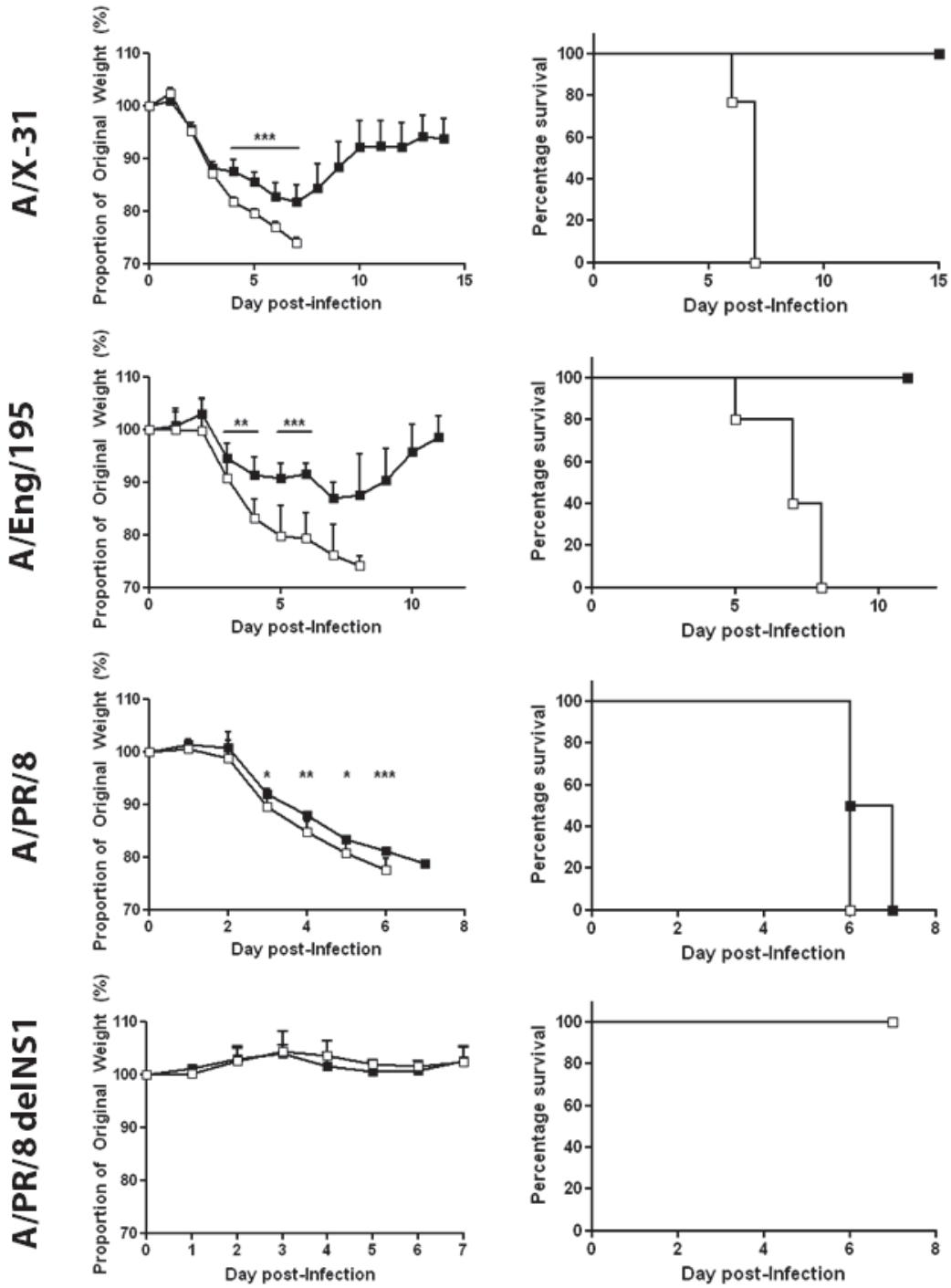

Figure 4.7: Weight loss and survival profiles of wild type and *Ifitm3*$^{-/-}$ mice infected with various influenza A subtypes. Mice were dosed as follows: A/X-31 (H3N2), 10^4 PFU; A/Eng/195 (A(H1N1)pdm09), 200 PFU; PR/8 (H1N1), 50 PFU; PR/8 delNS1 (H1N1), 10^3 PFU and monitored for the indicated time period, assessing daily for weight loss and morbidity. Mice that surpassed 25% weight loss were killed. ■: wild type, □: *Ifitm3*$^{-/-}$. Results show means ± S.D. (n > 5) Statistical significance was assessed by ANOVA (*: $p < 0.05$, **: $p < 0.01$, ***: $p < 0.001$).

4.2.3.2 Viral burden and distribution

Mice infected with X-31 influenza virus were assessed for viral load within their lungs via plaque assay and systemically for signs of viremia by qPCR. As shown in Figure 4.8, peak viral load at day 2 post-infection showed no significant difference between wild type and *Ifitm3*$^{-/-}$ mice. However, virus persisted within the *Ifitm3*$^{-/-}$ lungs to give a 10-fold higher burden at day six post-infection ($p = 0.0001$). These differences were confirmed by qPCR for influenza NP RNA on days one and six post-infection; showing the same trend. Analysis of the blood, spleen, brain and heart revealed no signs of viral RNA in organs outside of the respiratory system.

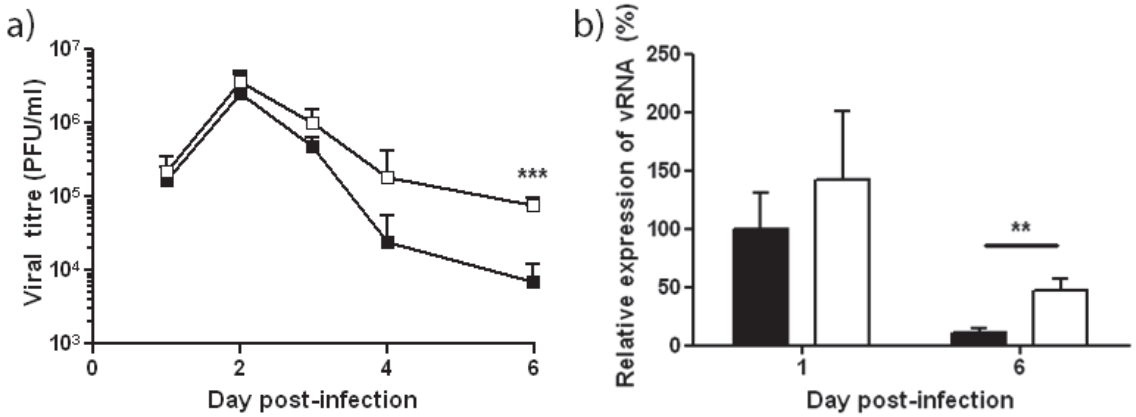

Figure 4.8: Lung viral burden over the course of influenza A virus infection. Results show the viral replication kinetics of X-31 influenza virus, as assessed by plaque assay (a). Results were verified by qPCR (b), wherein levels of NP expression were normalised to levels observed in wild type mice on day one post-infection. ■: wild type, □: *Ifitm3*$^{-/-}$. Results show means ± S.D. ($n > 4$). Statistical significance was assessed by Student's *t*-test (**: $p < 0.01$, ***: $p < 0.001$).

The distribution of virus within the lungs was analysed by immunohistochemistry (IHC) for both viral proteins (Figure 4.9a) and viral RNA (Figure 4.9b). RNA visualisation confirmed a much higher amount of vRNA within the lungs at day 6 post-infection in *Ifitm3*$^{-/-}$ mice; supporting the viral load quantification. Interestingly, protein IHC indicated *Ifitm3*$^{-/-}$ mice displaying more viral antigen deeper in the lung tissue than wild type littermates, where virus was restricted to large airways.

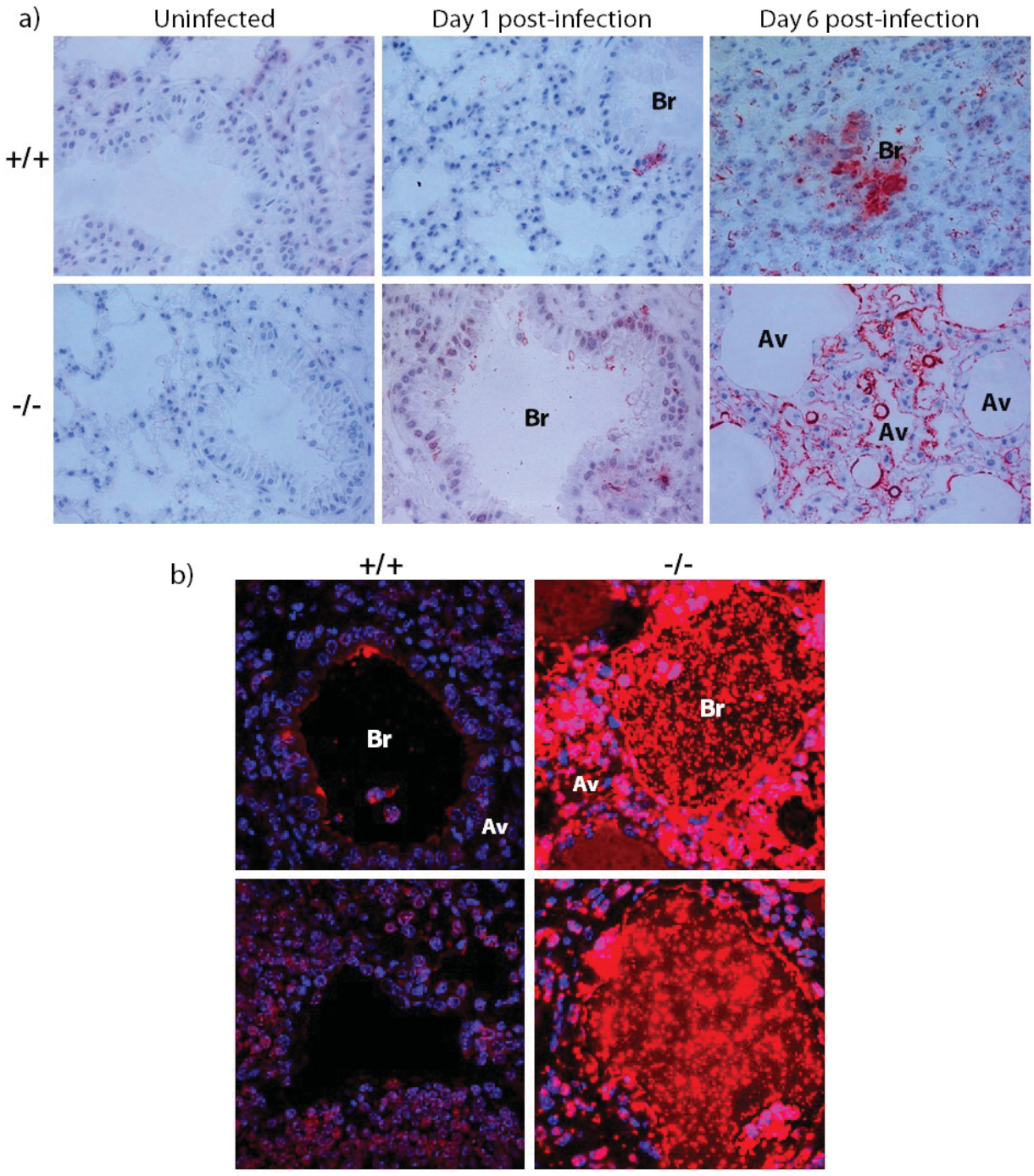

Figure 4.9: Viral antigen distribution through the lungs over the course of infection. Protein immunohistochemistry (a) over the course of infection showed the spread of virus in *Ifitm3*$^{-/-}$ lungs into the terminal bronchi and alveoli by day six post-infection, which was absent in wild type mice. At earlier time points there were no differences in virus distribution. Viral RNA immunohistochemistry (b) showed a greater abundance of vRNA on day 6 post-infection in *Ifitm3*$^{-/-}$ lungs, compared to wild type littermates (red: virus, blue: cell nuclei, Av: alveolus, Br: bronchiole). All images were taken at 20× magnification.

4.2.3.3 Pathology

Organs were removed over the course of infection and were assessed for pathological damage by a variety of means. Freshly excised *Ifitm3*$^{-/-}$ lungs showed signs of extensive damage, with multiple large lesions present on their surface at day 6 post-infection (Figure 4.10). Sectioning of *Ifitm3*$^{-/-}$ lungs revealed fulminant viral pneumonia, with severe inflammation, gross cellular infiltrate, oedema, red blood cell extravasation and hemorrhagic pleural effusion (Figure 4.10). Wild type mice showed moderate inflammation, with less extensive infiltration and oedema.

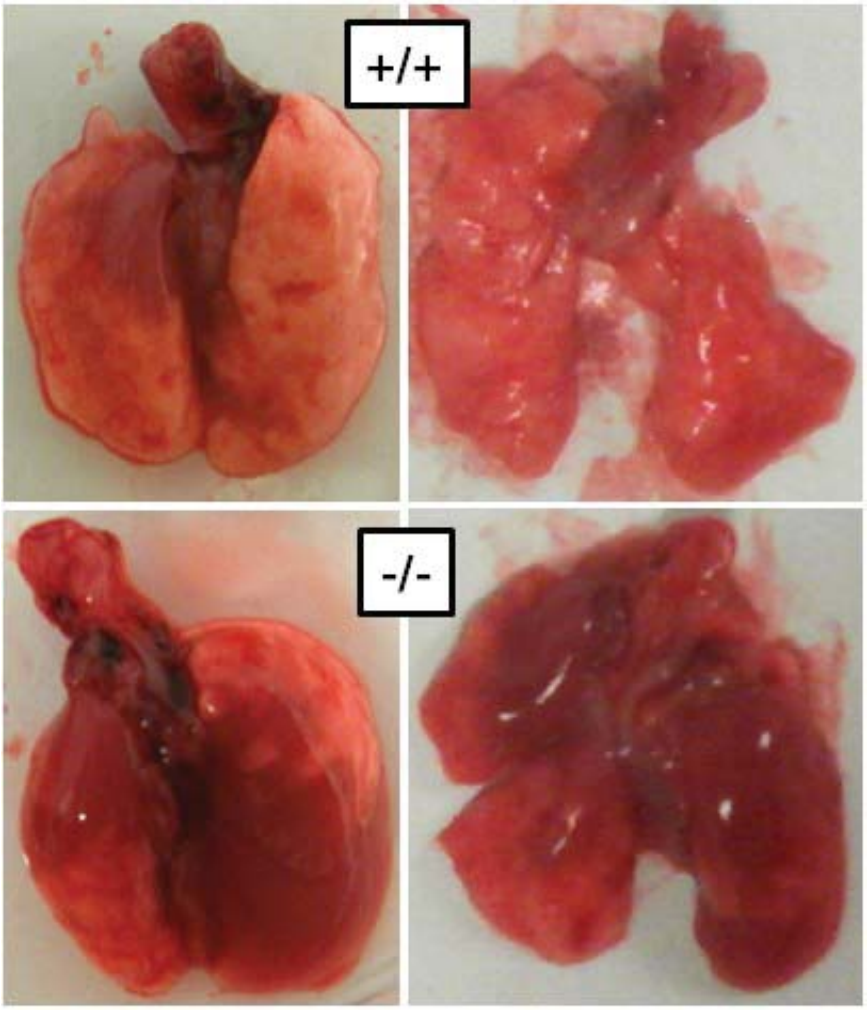

Figure 4.10: Gross lung pathology of mice following influenza A virus challenge. Mice were infected with X-31 influenza virus and pathological damaged assessed at day 6 post-infection. Gross pathology showed more extensive damage and several large lesions on the pleural surface of *Ifitm3*$^{-/-}$ lungs. Photos show distal views of the lungs with lobes as they are in-situ (left) and splayed (right) to reveal the extent of damage.

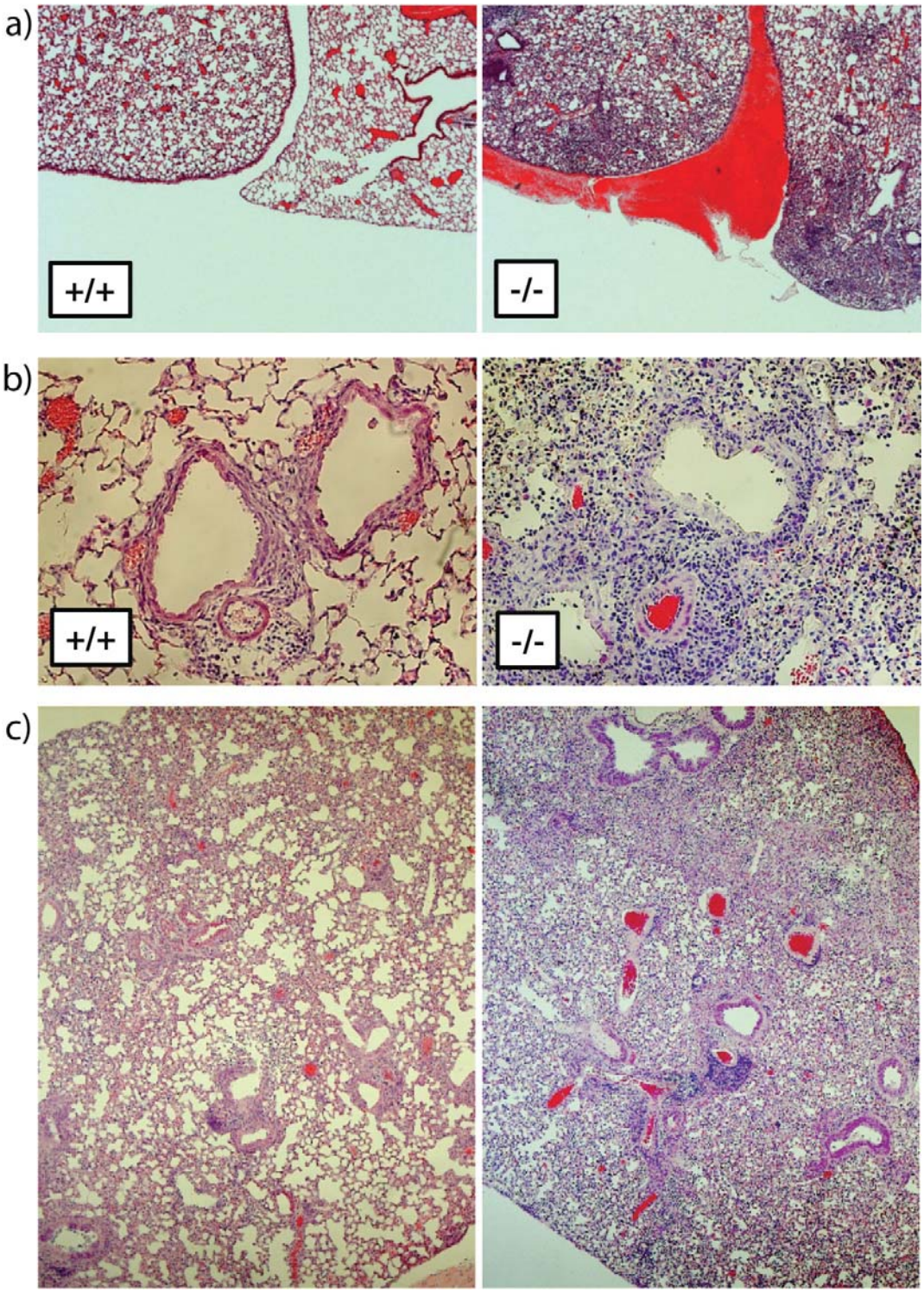

Figure 4.11: Lung sections of mice following influenza A virus challenge. Mice were infected with X-31 influenza virus and pathological damaged assessed at day six post-infection. Hemorrhagic pleural effusion (a), oedema, cell debris and cellular infiltrate (b, c) were also more pronounced in *Ifitm3*$^{-/-}$ lungs. Original magnification for (a) and (c), 5×, and for (b), 20×.

Furthermore, pathology was indirectly assessed by measuring lung weight. Excised respiratory systems were immediately cleaned and weighed to determine the extent of cellular infiltrate and water content present within the infected lungs on day six post-infection (Figure 4.12a). This revealed that *Ifitm3*$^{-/-}$ lungs were significantly heavier at the peak of morbidity, when compared to wild type littermates ($p = 0.0007$). Lungs were also removed and dried for seven days at 50^{o}C to investigate the amount of water present in the lungs at the same time point (Figure 4.12b). This showed that *Ifitm3*$^{-/-}$ mice had significantly more water in their lungs ($p = 0.02$); supporting the pathologically observed pneumonia.

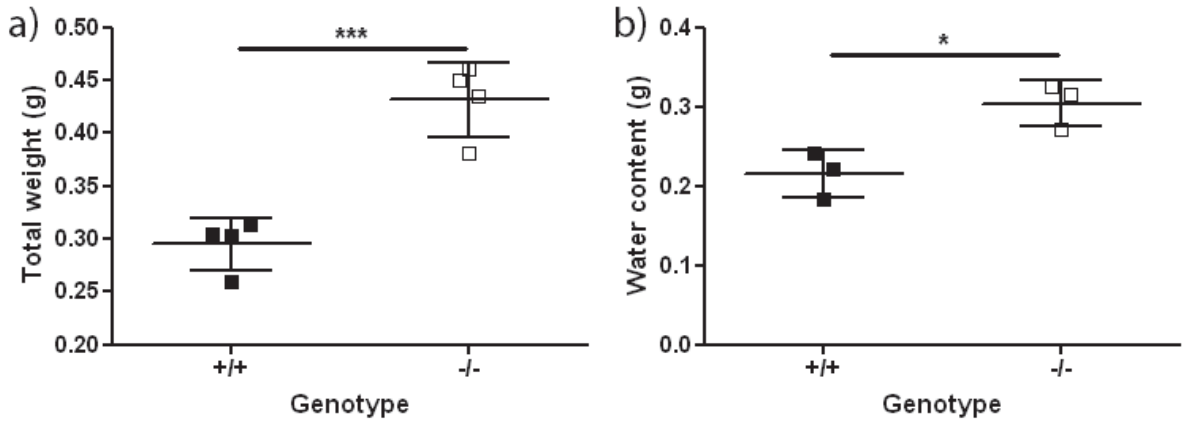

Figure 4.12: Total weight and water content of mouse lungs excised at day six post-influenza infection. Freshly removed lower respiratory systems (n = 4) trachea and lungs) were weighed to determine the extent of cellular and water infiltrate (a). Separately, lungs (n = 3) were dried for seven days and water content was calculated (b). ■: wild type, □: *Ifitm3*$^{-/-}$. Results show means ± S.D. Statistical significance was assessed by Student's *t*-test (*: $p < 0.05$, ***: $p < 0.001$).

Lungs were also assessed for necrotic and apoptotic damage using a terminal deoxynucleotidyl transferase dUTP nick end labelling (TUNEL) assay (Figure 4.13). This revealed extensive and widespread cell death across the breadth of the sectioned lobe in *Ifitm3*$^{-/-}$ mice. However, instances of such damage were isolated and limited in wild type littermates.

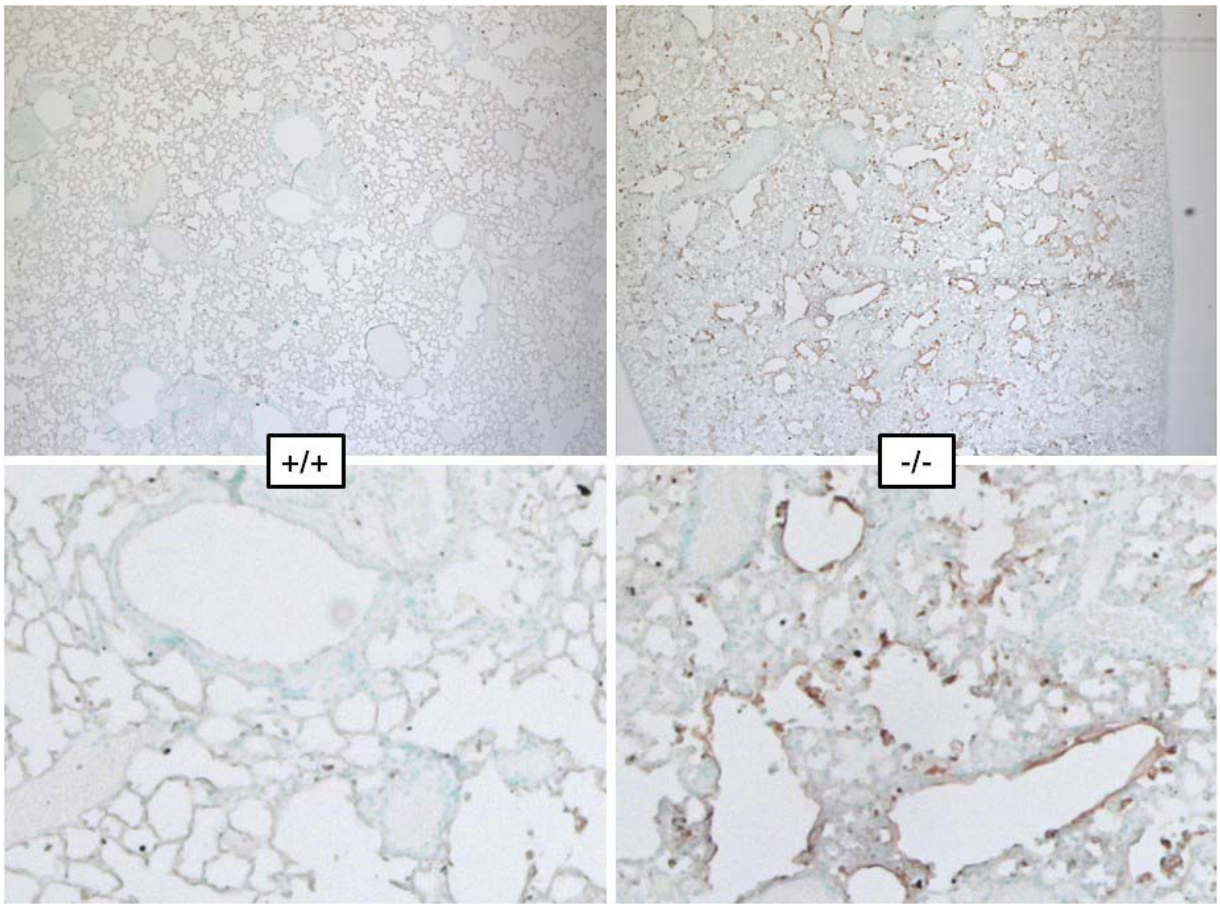

Figure 4.13: TUNEL assay for cell death in influenza-infected lungs. Lung sections from mice six days post-infection with influenza A were assayed for cell death. The assay revealed widespread and extensive damage across the entire love in *Ifitm3*$^{-/-}$ mice, but instances of such damage were limited and isolated in wild type control mice. Brown staining indicates the presence of DNA fragmentation, which is associated with apoptosis and necrosis. All cells have been counterstained with methyl green to aid visibility and contrast. Original magnification 5×.

4.2.3.3 Ifitm3 and osteopontin expression during infection

In order to monitor Ifitm3 expression over the course of infection, lungs were homogenised at set time points in order to assess whether expression was temporally regulated during viral infection. Western blot analysis qualitatively revealed that Ifitm3 expression increased over the course of infection up until day six post-infection in wild type mice (Figure 4.14a). Further to this, levels of osteopontin (Opn) were qualified by Western blot (Figure 4.14a) and quantified by ELISA (Figure 4.14b) and qPCR (Figure 4.14c). This was conducted owing to recent discoveries that Ifitm3 directly binds *Opn* mRNA and as such prevents its translation (El-Tanani *et al.* 2010). The ELISA and qPCR for osteopontin expression indicate there to be significantly more protein

present at day six post-infection ($p = 0.01$), and a trend towards elevated RNA levels ($p = 0.07$), at the time when Ifitm3 expression is typically highest. Interestingly, constitutive expression of Opn was also higher in uninfected animals.

Ifitm3 expression was also qualitatively examined *in vivo* through the use of IHC. Staining showed an up-regulation of Ifitm3 levels in infected lungs, compared to uninfected animals (Figure 4.15). Counterstaining for Ifitm1 also revealed that the ablation of Ifitm3 had no downstream effect on other Ifitm family members; thus confirming the specificity of the knockout.

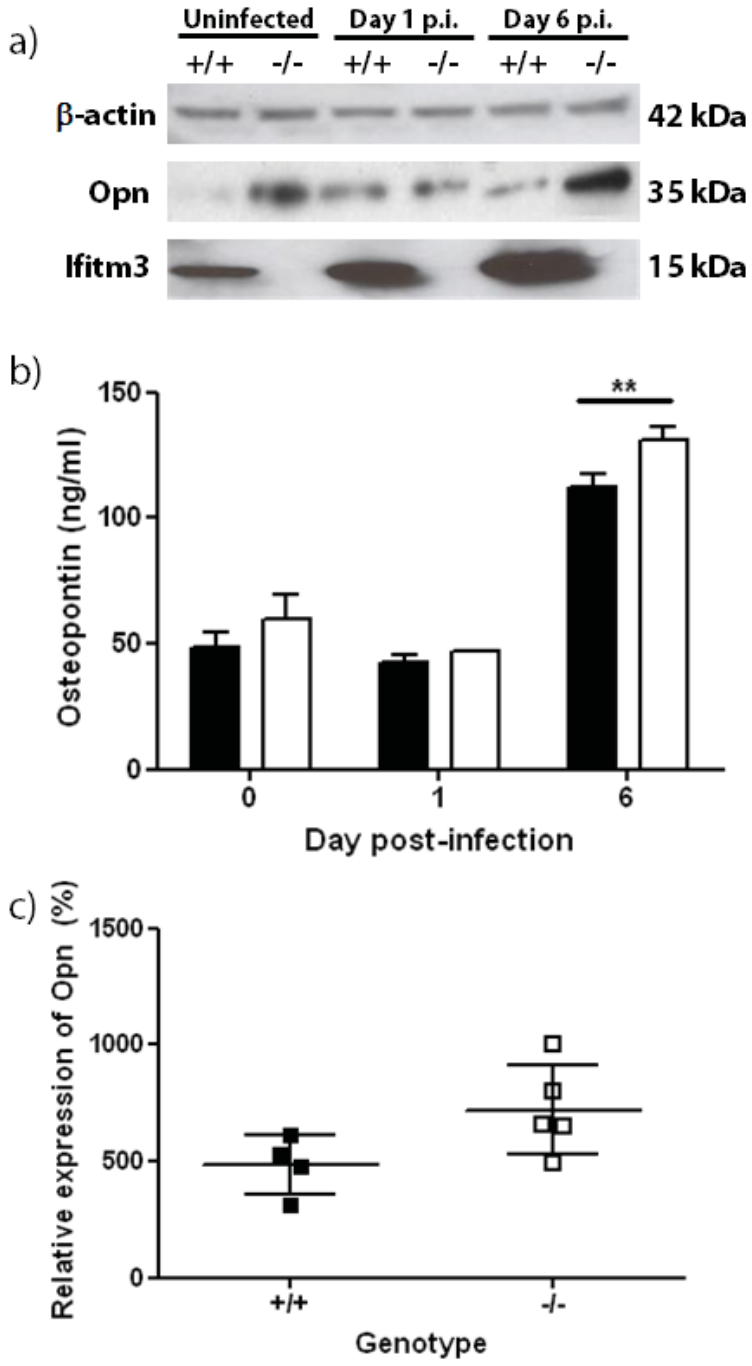

Figure 4.14: Expression levels of Ifitm3 and osteopontin over the course of infection. Western blot analysis showed Ifitm3 expression to increase over the duration of infection (a); similarly, osteopontin levels reached their highest levels in *Ifitm3*$^{-/-}$ mice at day six post-infection. This was confirmed by ELISA (b), which showed levels of Opn to be significantly higher than those observed in wild type mice. The trend was also apparent at the RNA level on day six post-infection (c), where expression was normalised to uninfected animals' *Opn* levels. ■: wild type, □: *Ifitm3*$^{-/-}$. Results show means ± S.D. ($n > 4$). Statistical significance was assessed by Student's *t*-test (**: $p < 0.01$).

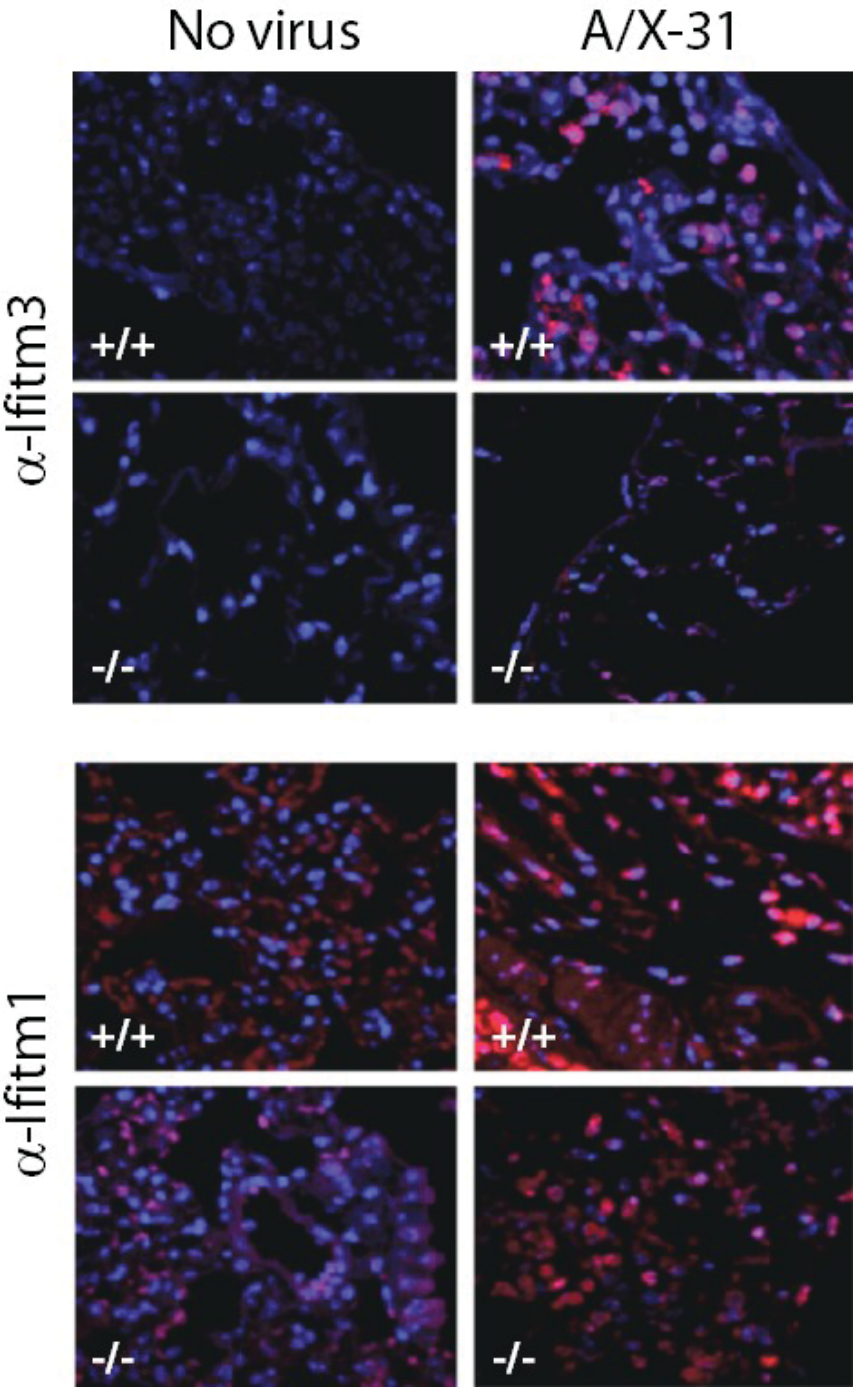

Figure 4.15: Expression of Ifitm1 and Ifitm3 in mouse lungs with or without influenza infection. Lung sections from wild type and *Ifitm3*$^{-/-}$ mice at two days post-A/X-31 infection were stained to assess the expression of Ifitm3 and Ifitm1 (both red). Tissue was counterstained for DNA (blue). Viral infection is shown to up-regulate both Ifitm1 and Ifitm3 in lungs, but the loss of Ifitm3 does not influence Ifitm1 expression.

4.2.3.3 Immunology

4.2.3.3.1 Cellular response: respiratory system

The leukocyte response to viral infection is crucial to defence against influenza virus infection (discussed in section 1.4.1.3). To examine the cellular response, lungs were excised, homogenised and cells stained for a variety of cell types over the course of infection. Total cell numbers in the bronchoalveolar lavage (BAL) fluid and lung tissue were calculated to quantify the extent of cellular infiltrate seen in pathology sections (Figure 4.11). Counts showed there to be significantly more leukocytes present in the BAL of *Ifitm3*$^{-/-}$ mice, six days post-infection ($p = 0.001$) (Figure 4.16a). Similarly, there was a trend for larger leukocyte numbers in total in the lungs at the same point of infection ($p = 0.06$) (Figure 4.16b).

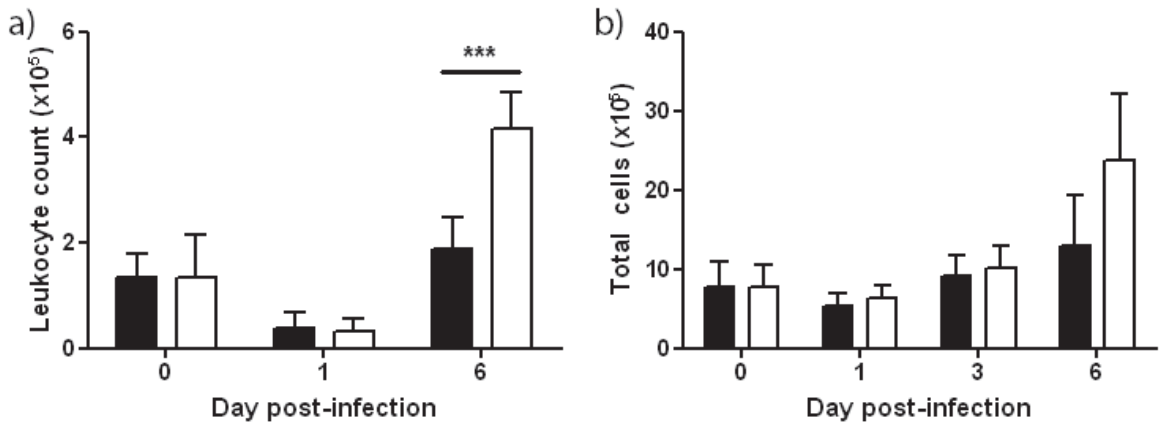

Figure 4.16: Respiratory system cell counts during influenza infection. Live cells were counted in either BAL (a) or total homogenised lung (b) at the indicated time points following challenge with A/X-31 influenza virus. ■: wild type, □: *Ifitm3*$^{-/-}$. Results show means ± S.D. ($n > 4$). Statistical significance was assessed by Student's *t*-test (***: $p < 0.001$).

Leukocytes were further characterised by flow cytometry to qualify the contribution of various cell subtypes in the immune response to influenza virus in *Ifitm3*$^{-/-}$ mice. Analysis showed that during the early infection stage (days 1-3) there were minor differences in the major immune cell populations between the genotypes of mice, with elevated numbers of neutrophils ($p = 0.05$) and NK cells ($p = 0.02$) on days one and three, respectively. However, at day six post-infection there was significant evidence of lymphopenia, with reductions in CD4 T-cell ($p = 0.004$), CD8 T-cell ($p = 0.02$) and NK cell ($p = 0.0001$) populations in the lungs of *Ifitm3*$^{-/-}$ mice, which was

accompanied by significantly higher numbers of neutrophils (p = 0.007) compared to wild type mice (Figure 4.17).

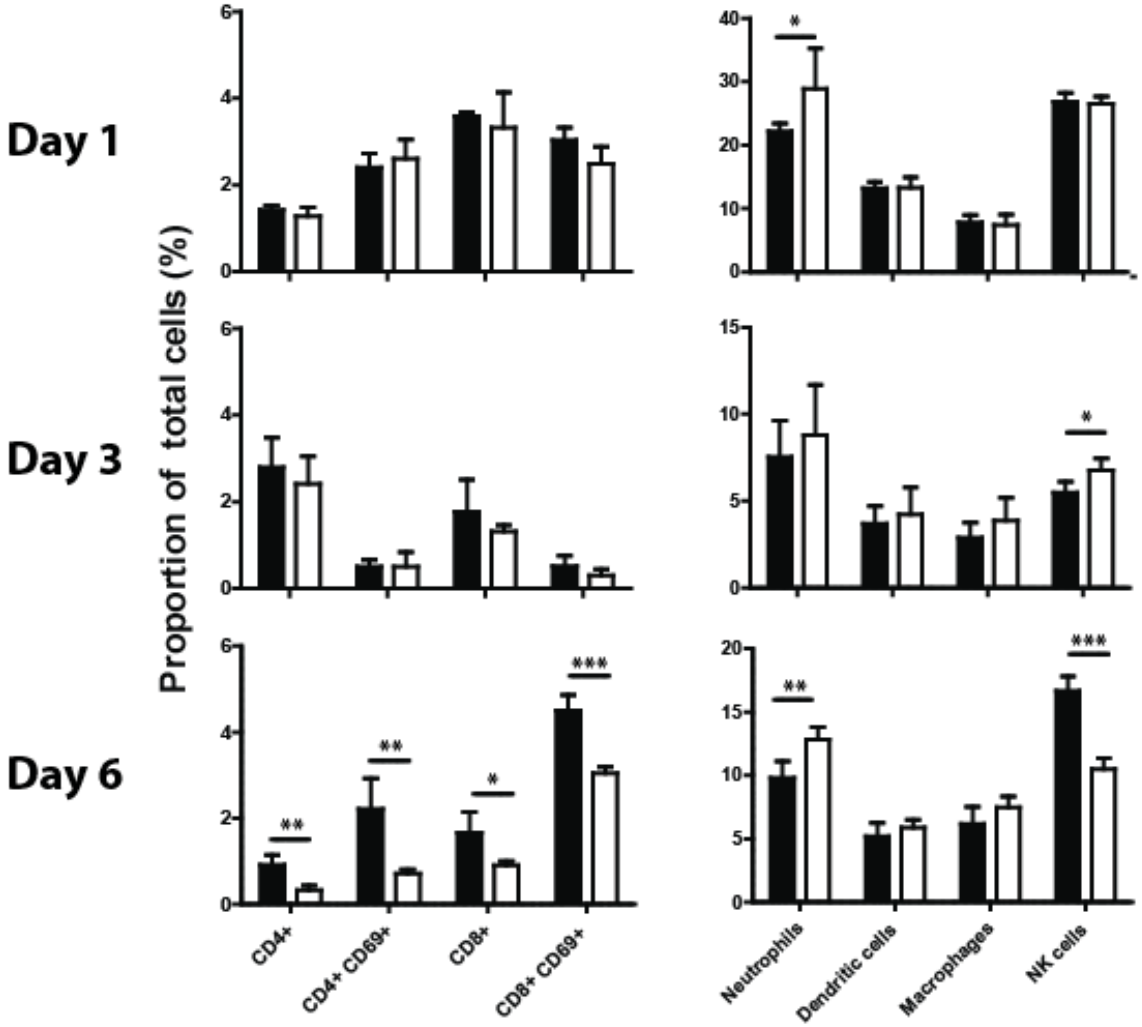

Figure 4.17: Immune cell populations over the course of influenza virus infection. Lungs were excised, homogenised and analysed by flow cytometry to quantify the contribution of various cellular subtypes at the indicated times post-infection. Widespread significant differences were observed on day six post-infection, wherein lymphopenia and an excess of neutrophils are seen. ■: wild type, □: *Ifitm3*$^{-/-}$. Results show means ± S.D. (n > 4). Statistical significance was assessed by Student's *t*-test (*: p < 0.05, **: p < 0.01, ***: p < 0.001). .

4.2.3.3.2 Cellular response: systemic

In order to quantify the systemic immune response to infection, mice were either killed by cardiac puncture and total leukocyte counts were calculated (Figure 4.18a), or mice were bled by

tail vein puncture and blood smears taken to analyse blood differential cell counts and quantify the levels of leukocytes, polymorphonuclear (PMN) cells and monocytes during infection (Figure 4.18b). The results of the total leukocyte count revealed that *Ifitm3*$^{-/-}$ mice were largely unresponsive and failed to show the early peak in leukocyte numbers on day two post-infection. Similarly, *Ifitm3*$^{-/-}$ mice showed a significantly lower number of leukocytes in circulation on day six post-infection when compared with wild type littermates ($p = 0.005$). Significant lymphopenia was also observed on day two post-infection ($p = 0.04$), with a reduction in the number of circulating lymphocytes.

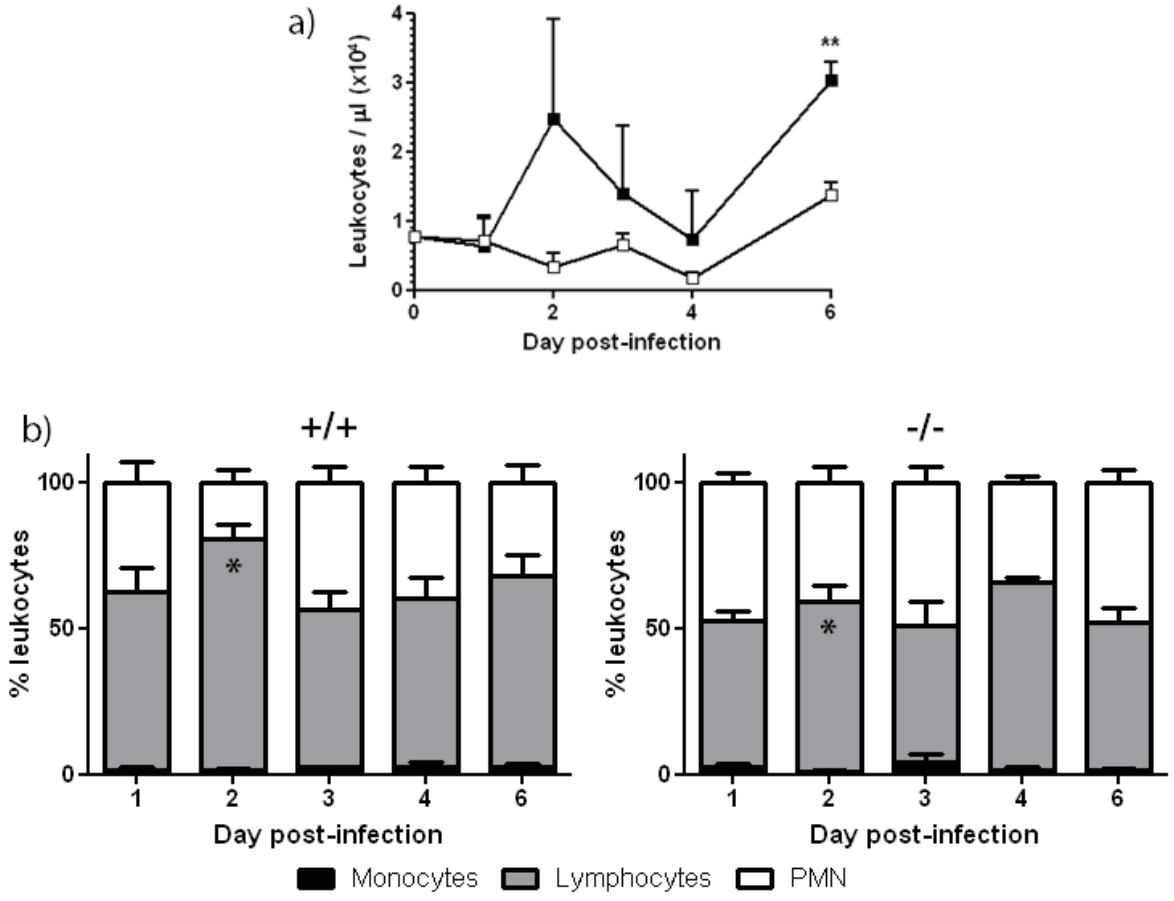

Figure 4.18: Systemic leukocyte responses to influenza virus infection. Total leukocyte counts (a) were taken by cardiac puncture of >3 mice per genotype at the indicated time points post-infection. Blood differentials (b) were calculated in a blinded fashion by assessing leukocyte populations on blood smears collected by tail vein puncture from >4 mice per genotype. ■: wild type, □: *Ifitm3*$^{-/-}$. Results show means ± S.D. Statistical significance was assessed by Student's *t*-test (*: $p < 0.05$, **: $p < 0.01$).

4.2.3.3.3 Cytokine response

Cytokines, along with immune cell populations, are one of the key mediators of the immune response to invading pathogens. Additionally, they can also be responsible for the immunopathology associated with severe disease, as discussed in section 1.4.4. *Ifitm3*$^{-/-}$ mice differed in their cytokine cascades when compared with wild type mice, generally showing a more exaggerated response. Some of the most important deviations were observed with the pro-inflammatory cytokines IL-6, TNFα, G-CSF and MCP-1 (Figure 4.19a); all of which were significantly up-regulated over the course of infection. A further 11 inflammatory and anti-inflammatory cytokines were also assessed by bead-based Luminex assay over the course of infection (Figure 4.19b), which showed a similarly exaggerated trend.

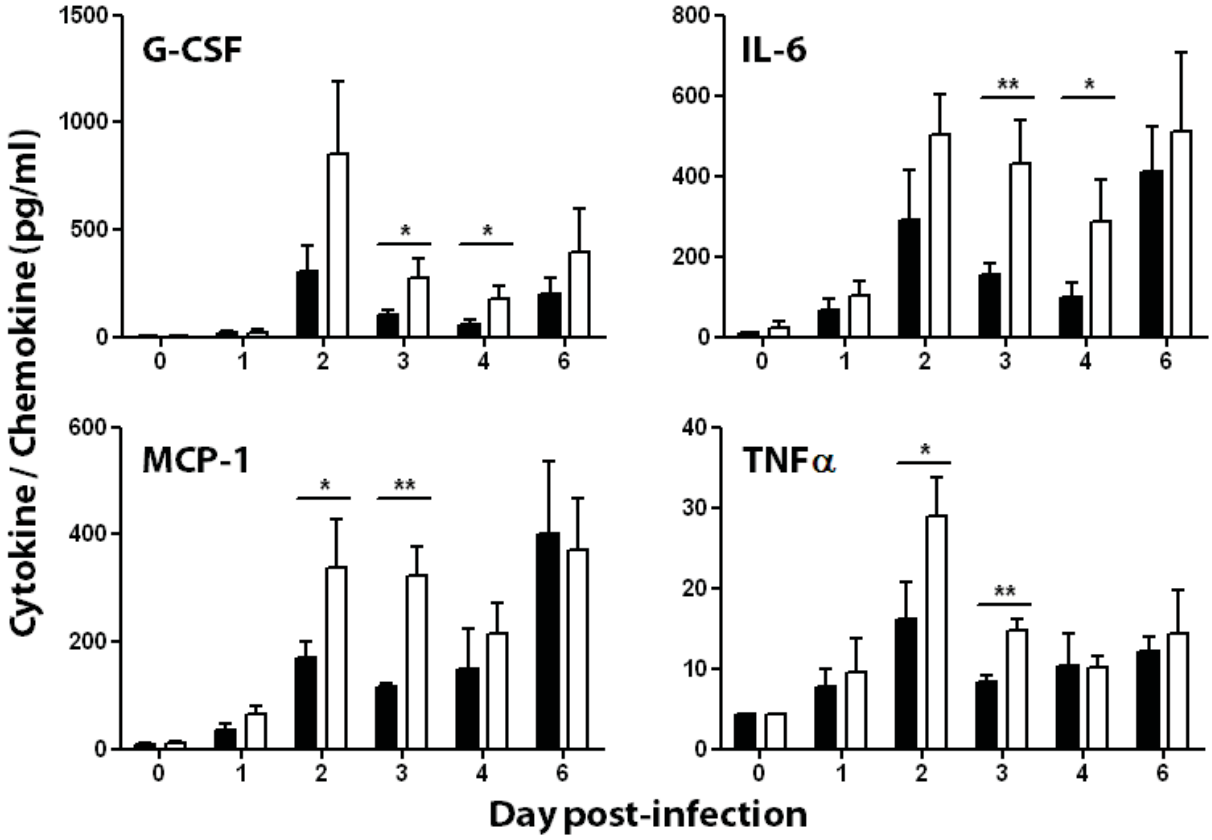

Figure 4.19a: Cytokine responses in the lungs of mice infected with influenza virus. Concentrations of a panel of cytokines present in the lungs over the course of A/X-31 infection were measured by Luminex assay. ■: wild type, □: *Ifitm3*$^{-/-}$. Results show means ± S.D. Statistical significance was assessed by Student's *t*-test (*: $p < 0.05$, **: $p < 0.01$).

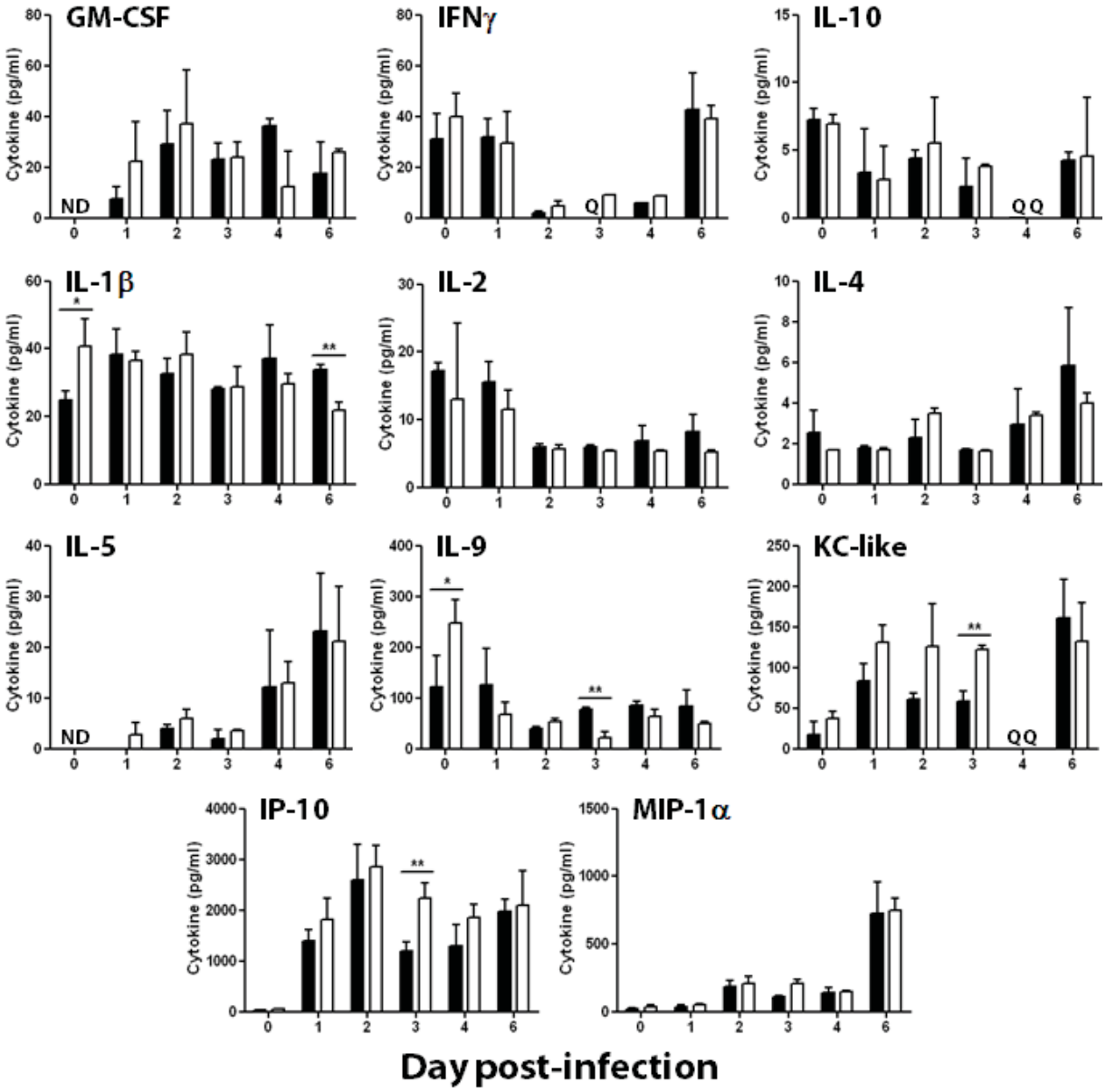

Figure 4.19b: Cytokine responses in the lungs of mice infected with influenza virus. Concentrations of a panel of cytokines present in the lungs over the course of A/X-31 infection were measured by Luminex assay. Q = <50 beads detected, therefore recorded as quality control failure, ND = not detected. ■: wild type, □: *Ifitm3*$^{-/-}$. Results show means ± S.D. Statistical significance was assessed by Student's *t*-test (*: $p < 0.05$, **: $p < 0.01$).

4.2.3.3.4 Adoptive bone marrow transfer

To evaluate the relative contribution of the immune system against influenza in *Ifitm3*$^{-/-}$ mice, adoptive bone marrow transfer was conducted. Both wild type and *Ifitm3*$^{-/-}$ mice were irradiated and bone marrow was transferred between animals to create chimeras (henceforth termed wt^{BM-}

Ifitm3: wild type mice with *Ifitm3*$^{-/-}$ bone marrow, and Ifitm3$^{BM\text{-}wt}$): *Ifitm3*$^{-/-}$ mice with wild type bone marrow). Mice that survived for 10 days post-transfer were deemed to have been successfully repopulated with immune progenitor cells and were infected with A/X-31 influenza after eight weeks and recorded for phenotypic differences (Figure 4.20).

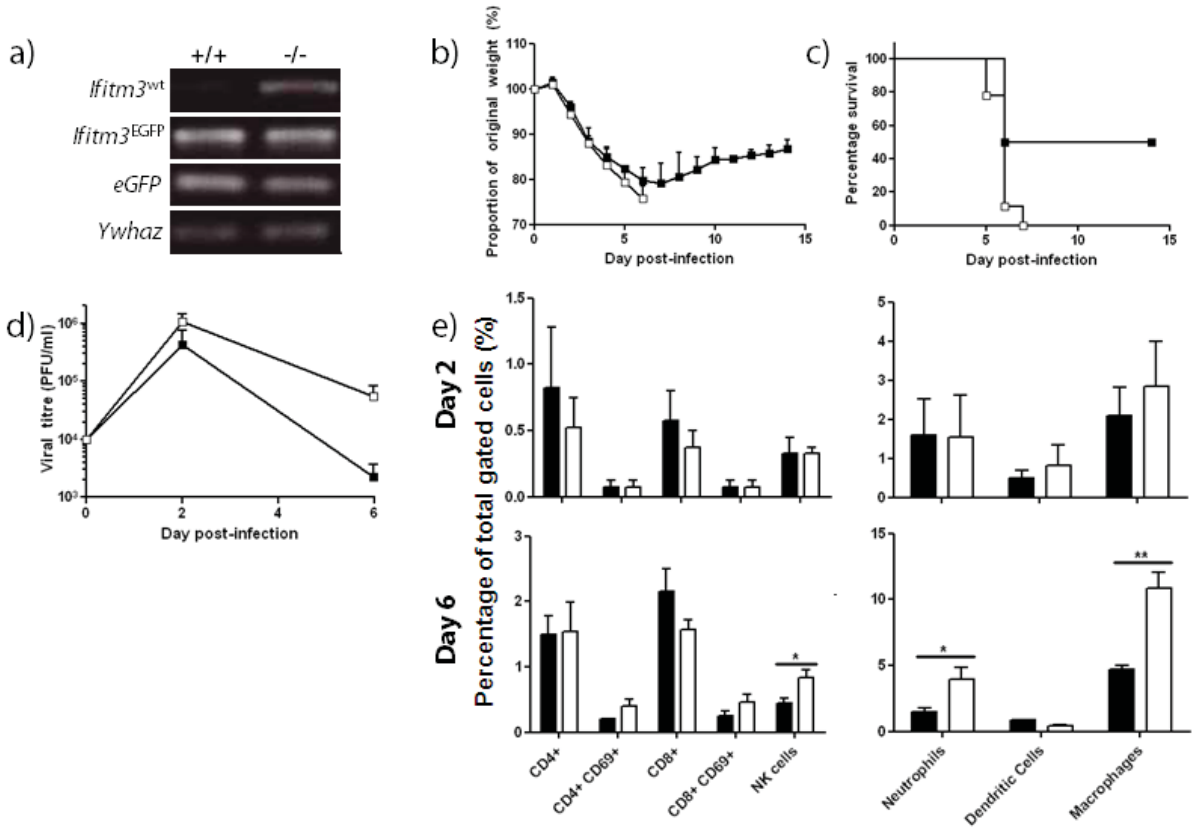

Figure 4.20: Influenza challenge of chimeric mice. Wild type and *Ifitm3*$^{-/-}$ mice were irradiated and bone marrow was transferred between genotypes to create chimeras. Spleens were excised from animals and analysed by PCR for the presence of the wild type *Ifitm3* allele (*Ifitm3*^{wt}), *Ifitm3*$^{-/-}$ allele (*Ifitm3*^{EGFP}) and *eGFP*, with *Ywhaz* included as a reference loading gene (a). Mice were infected with 10^4 PFU of A/X-31 and weight loss and survival recorded for 14 days post-infection (b,c). Lungs were removed on days two and six post-infection to quantify viral load (d) and resident immune cell populations (e). ■: wt$^{BM\text{-}Ifitm3}$, □: Ifitm3$^{BM\text{-}wt}$. Results show means ± S.D. (n > 3). Statistical significance was assessed by Student's *t*-test (*: $p < 0.05$, **: $p < 0.01$).

To verify the chimeras, spleens were removed and PCR analysis conducted for wild type and *Ifitm3*^{EGFP} allele presence in both sets of mice. This confirmed that both sets of mice had become successfully reconstituted with the donor's bone marrow (Figure 4.20a). qPCR analysis of these samples revealed that wt$^{BM\text{-}Ifitm3}$ mice contained 28× more Ifitm3^{EGFP} DNA than knockout mice,

whilst Ifitm3$^{BM\text{-}wt}$ mice contained 10× more *Ifitm3*^{wt} DNA than wild type mice in their spleens (data not shown).

Infection of the chimeric mice with influenza virus resulted in >20% weight loss in both genotypes of mice (Figure 4.20b), with 100% mortality in the Ifitm3$^{BM\text{-}wt}$ group, and 50% mortality in the wt$^{BM\text{-}Ifitm3}$ group (Figure 4.20c). Viral kinetics in both sets of mice were the same as those observed in non-chimeric challenges (Figure 4.7), with Ifitm3$^{BM\text{-}wt}$ mice showing slower resolution of viral infection, with a >10-fold higher viral burden on day six post-infection (Figure 4.20d). Significant differences were observed on day six post-infection, with Ifitm3$^{BM\text{-}wt}$ mice having significantly more NK cells ($p = 0.03$), neutrophils ($p = 0.04$) and macrophages ($p = 0.006$) present in their lung tissue.

4.2.4 Collaborative work on human IFITM3 genetics[1]

To assess the IFITM3 allelic diversity in humans, samples were collected from patients hospitalised with confirmed influenza virus infections during the 2009-2010 H1N1 pandemic. These patients were all Caucasians with no known co-morbidities. A total of 53 DNA samples were collected in association with the *MOSAIC* and *GenISIS consortia* from England and Scotland, which were then subsequently sequenced. These were aligned to the human *IFITM3* encoding reference sequence (Acc. No.: NC_000011.9) and Phred values compared.

Significant deviations in some of the sequenced samples from the human reference sequence occurred at DNA position 320772, which encodes SNP rs12252, wherein a majority T is mutated to a minority C. In total, we found 46 TT, 4 TC, and 3 CC individuals (Figure 4.21a). In collaboration with others at the WTSI and Roslin Institute in Edinburgh, we found the genotypes associated with rs12252 differed significantly from ethnically matched Europeans in the 1000 Genomes sequence data and from genotypes imputed against the June 2011 release of the 1000 Genomes phased haplotypes from the UK, Netherlands and Germany (Table 4.1). Patients' genotypes also depart from Hardy Weinberg equilibrium (p=0.003), showing an excess of C

[1]Collaboration was sought to complete the human genetics component of the IFITM3 work. Sarah E. Smith sequenced the patients' *IFITM3* genes and scored Phred values; Aarno Palotie and Verneri Anttila performed 1000 Genomes analyses and imputation of SNPs; Chris Tyler-Smith performed evolutionary analyses on the *IFITM3* allele; and J. Kenneth Baillie performed principle component analyses.

alleles in this population (Figure 4.21a). Principal components analysis of over 100K autosomal SNPs showed no evidence of a hidden population structure differences between WTCCC controls and a subset of the hospitalised individuals from this study (Figure 4.21b). Further collaboration with Chris Tyler-Smith's group at the WTSI showed evidence for positive selection on the *IFITM3* locus in human populations acting over the last tens of thousands of years in Africa (Figure 4.21c).

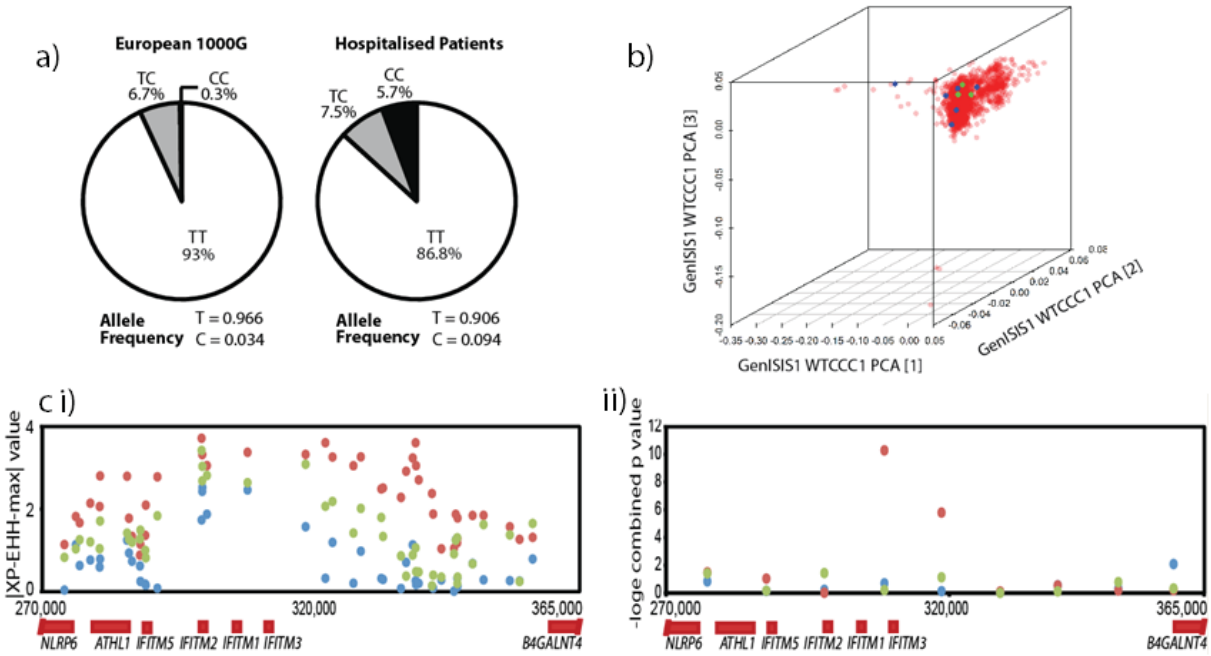

Figure 4.21: Single nucleotide polymorphisms of the human *IFITM3* gene and the prevalence of SNP rs12252. Sequencing of patients hospitalised with influenza virus during the 2009-2010 influenza pandemic showed an overrepresentation of individuals with the minority C allele at SNP rs12252. Principle component analyses (b) were conducted to check for clustering of a selection of TT (blue circles) and TC / CC (green circles) samples against 1499 controls from the WTCCC 1958 Birth Cohort (red circles). Positive selection analysis were conducted using a haplotype-based test (|XP-EHH-max|, (ci) where data points above 2.7 in the YRI (red), 3.9 in the CEU (blue) and 5.0 in the CHB+JPT (green) are in the top 1% of values and using a combination of three allele frequency spectrum-based test statistics, namely Tajima's D, Fay and Wu's H and Nielsen *et al.*'s CLR (cii), on 10 kb windows along chromosome 11 encompassing the *IFITM3* locus. Evidence for positive selection is seen only in the YRI.

Table 4.1: Allele and genotype distribution derived from multiple global populations of the 1000 Genomes Project and patients hospitalised with influenza for SNP rs12252 of IFITM3.

Population	Allele Frequency		Genotype			Total	HW[1]	P-value[5]
	C	T	CC	CT	TT	Samples		
YRI[2]	0.093	0.907	1	9	49	59	0.40	-
CHB/JPT[2]	0.3	0.7	9	18	33	61	0.03	-
CEU/FIN/GBR/IBI/TSI[2]	0.036	0.964	1	24	335	360	0.37	-
Hospitalised patients[3]	0.094	0.906	3	4	46	53	0.003	-
WTCCC1[4]	0.028	0.972	-	-	-	2938	0.73	6.46×10^{-5}
Netherlands[4]	0.026	0.974	-	-	-	8892	0.67	1.11×10^{-5}
Germany[4]	0.029	0.971	-	-	-	6253	0.82	6.93×10^{-5}

[1] Probability that observed genotype frequencies depart from Hardy-Weinberg equilibrium.
[2] Allele and genotype frequencies obtained from 1000 Genomes sequence data, (YRI, African ancestry, CHB/JPT, Chinese and Japanese ancestry, CEU/FIN/GBR/IBS/TSI, European ancestry).
[3] Allele and genotype frequencies determined in this study.
[4] Allele frequencies determined in this study imputed against the June 2011 release of 1000 Genomes phased haplotypes.
[5] P-value for additive model association analysis of hospitalised patients vs. the population samples, using SNPTEST v2.1.1.

4.2.5 Restrictive capacity of truncated and rs12252-C containing IFITM3

The rs12252-C SNP is purported to act as a splice site acceptor site, which in turn would truncate the full length IFITM3 protein at its N-terminal by 21 amino acids (NΔ21). In collaboration with Abraham L. Brass, Harvard University, plasmids encoding either the full length or NΔ21 DNA sequence were transduced into A549 cells to examine the effect of the loss of the terminal 21 amino acids at the N-terminal. Cells were confirmed to be stably expressing either of the constructs by Western blot (Figure 4.22a) and were subsequently challenged with four strains of influenza virus (A/WSN/33, A/California/07/2009, A/Uruguay/716/2007 and B/Brisbane/60/2008). Viral NP expression was quantified 12 hours post-infection (Figure 4.22b). The *in vitro* assays showed that NΔ21 IFITM3 confers minimal restrictive capacity, whilst full length IFITM3 was capable of significantly restricting all strains of influenza A and B tested.

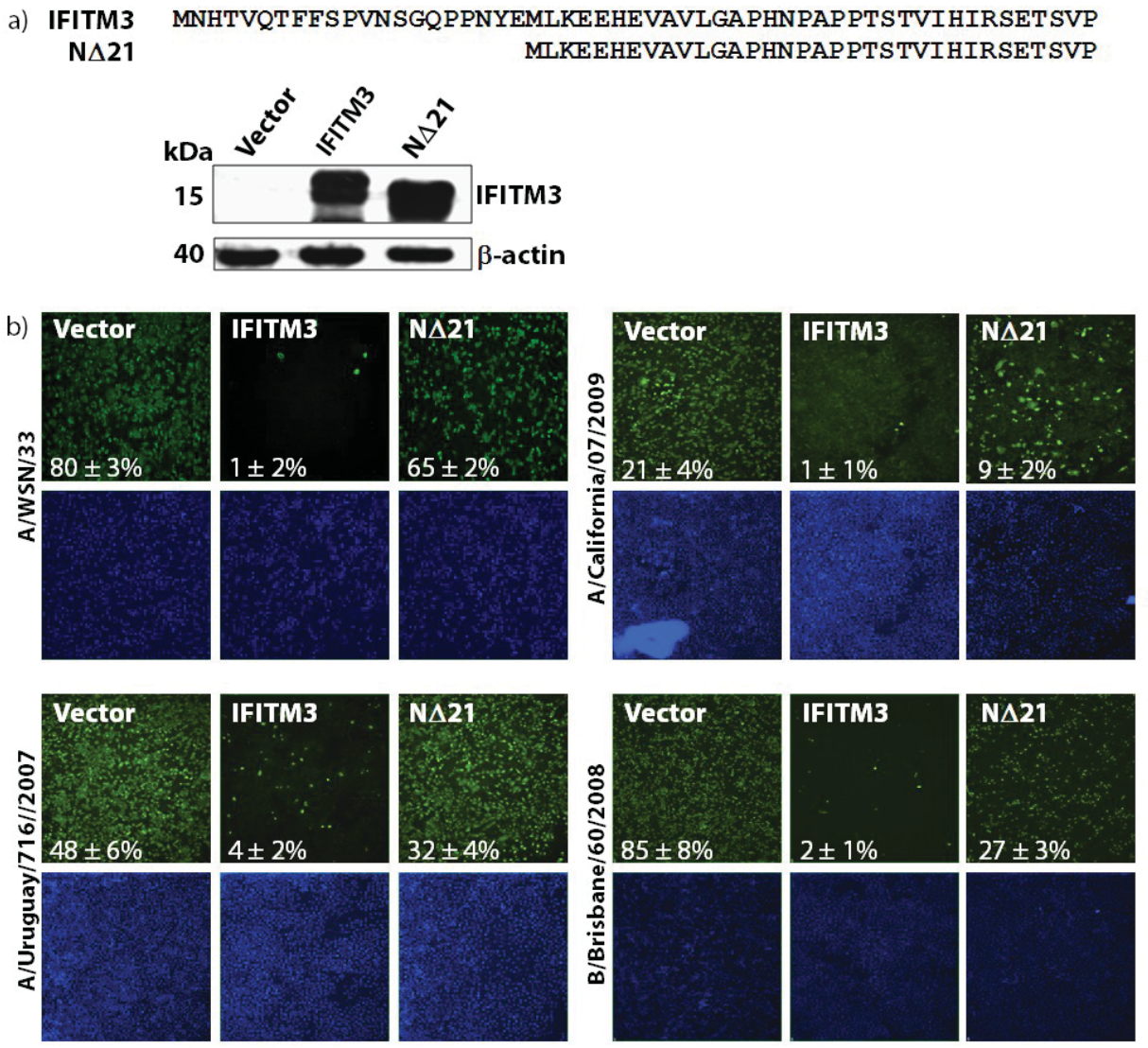

Figure 4.22: Impact of IFITM3 NΔ21 truncation on restriction of influenza A and B viruses. A549 cells were transduced with plasmids to express either empty vector control (Vector), full-length IFITM3 (IFITM3), or an N-terminally truncated IFITM3 (NΔ21) protein. Expression was confirmed by Western blot (a). Cells were subsequently infected with the indicated strains of influenza virus (b) and were assayed after 12 hours for influenza NP expression. Green: influenza NP expressing cells, blue: DAPI staining of cells. Results show mean level of infection ± S.D. (n = 3).

To assess the function of the rs12252-C SNP, human lymphoblastoid cell lines (LCLs) were sequenced to identify those containing the rs12252-T and rs12252-C alleles. These were subsequently infected with WSN/33 influenza A virus to determine viral susceptibility. As shown in Figure 4.23, the presence of CC resulted in increased susceptibility to influenza virus

infection in both an unstimulated and IFN-induced environment. Furthermore, Western blot analysis showed that IFITM3 expression was lower in rs12252-C containing LCLs in the latent state. However, IFN stimulation resulted in a qualitatively similar level to that of the rs12252-T containing LCLs.

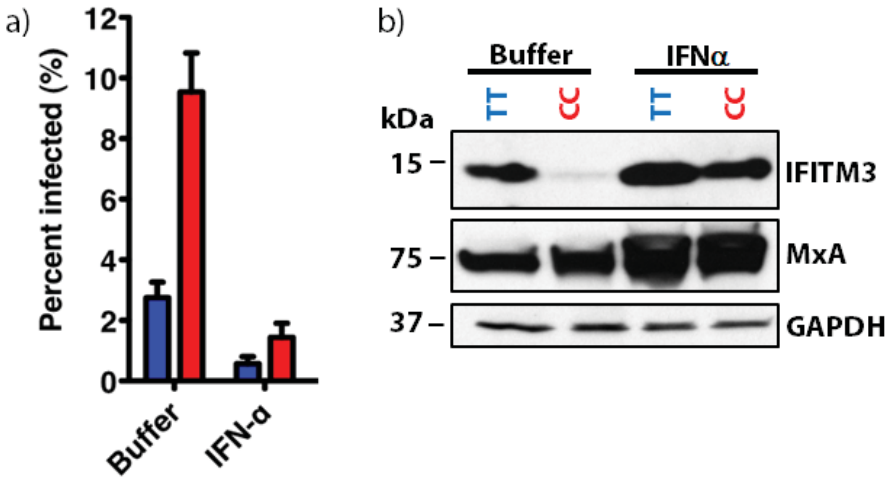

Figure 4.23: Viral replication and IFITM3 expression in rs12252-TT and rs12252-CC containing human cells. LCLs homozygous for either the majority T (blue) or minority C (red) alleles were challenged with WSN/33 influenza with or without IFN stimulation (a). Western blots for these LCLs were also conducted (b) and probed for IFITM3 expression, MxA for assessment of ISG expression and GAPDH as a housekeeping loading control. Results show means ± S.D. (n = 3).

4.3 Discussion

This study showed that Ifitm3 is a crucial antiviral restriction factor necessary for resistance to influenza virus in mice. The loss of Ifitm3 results in a persistent viral infection in the lungs, and the onset of fulminant viral pneumonia when mice are challenged with a low pathogenicity strain of influenza virus, which subsequently results in heightened morbidity and mortality. Furthermore, these studies showed for the first time that influenza resistance and susceptibility may have a heritable component in humans, with the enrichment of SNP rs12252 in a cohort of hospitalised patients suggesting that defects in IFITM3 may result in a more severe disease phenotype. This SNP is thought to act as a splice site acceptor, which truncates IFITM3 at its N-terminus by 21 amino acids (NΔ21). This study shows that this mutation greatly reduces the antiviral activity of IFITM3.

Typically, low pathogenicity (LP) influenza viruses, such as A/X-31 and A/Eng/195 cause mild weight loss and are largely asymptomatic in wild type mice, at the doses used here (Mozdzanowska *et al.* 2000; Guo *et al.* 2011; Vlahos *et al.* 2011). They do not normally cause extensive viral replication throughout the lungs, or cause the cytokine dysregulation and death typically seen after infection with highly-pathogenic (HP) viral strains (Belser *et al.* 2010). However, *Ifitm3*$^{-/-}$ mice became moribund and showed severe signs of clinical symptoms by day six post-infection, as a result of delayed viral clearance, extensive respiratory tissue damage and fulminant viral pneumonia, which subsequently resulted in death. It therefore appears as though the removal of a functional Ifitm3 protein enables a typically LP influenza virus to elicit symptoms more commonly associated with HP infections.

Indeed, experiments using the HP 1918 'Spanish' influenza strain and avian H5N1 strains have resulted in severe pathological damage and death in a range of animals, including mice and primates (Tumpey *et al.* 2005a; Kobasa *et al.* 2007; Maines *et al.* 2008). Further to the extensive pathological damage caused by these viruses, several other symptoms seen in the current study would also more commonly be associated with HP influenza infection. One of the notable features seen in the study was the depletion of NK, CD4+ and CD8+ lymphocytes both within the lungs and systemically. T-cells are seen as crucial in the clearance of influenza virus from the body (Schmolke and García-Sastre 2010; Zhang and Bevan 2011); therefore making their absence counterintuitive. However, lymphopenia has been noted in HP (but not LP) influenza infections in both animals and humans (Tumpey *et al.* 2000; Maines *et al.* 2008; Perrone *et al.* 2008; Belser *et al.* 2010); although the reasoning as to why this depletion occurs is currently unknown.

In addition to the leukopenia and lymphopenia, two other traits associated with HP infections are dysregulated cytokine production and excessive cellular infiltrate into the lungs during infection; both of which were seen in the current study. The observed exaggerated pro-inflammatory responses in the lungs of *Ifitm3*$^{-/-}$ mice are particularly noteworthy, with higher levels of TNFα, IL-6, G-CSF and MCP-1 showing the most marked changes. This is indicative of the extent of viral spread within the lungs, as TNFα and IL-6 are released from cells upon infection (Julkunen *et al.* 2000). Consistent with the pathological damage, these changes are comparable in level to

those observed in non-H5N1 HP influenza infections (Belser *et al.* 2010). A novel observation was the elevated levels of osteopontin (Opn) in the lungs following influenza infection. Opn, which can act as a neutrophil chemoattractant (Nishimichi *et al.* 2011), is up-regulated in severe acute respiratory syndrome coronavirus (SARS-CoV) infections (Smits *et al.* 2011) and has been shown to directly but inversely interact with IFITM3 (El-Tanani *et al.* 2010). Thus, it is interesting that elevated expression of Opn correlates with an increase in cellular infiltrate, especially neutrophils, in the airways on day six post-infection (Figure 4.14). Such heightened levels may be contributing to neutrophil accumulation in the lungs. Neutrophil chemotaxis, together with elevated proinflammatory cytokine secretion, has previously been reported as one of the primary causes of acute lung injury (Yum *et al.* 2001; Grommes and Soehnlein 2011; Narasaraju *et al.* 2011). Similarly, the observed elevated levels of Opn in uninfected mice may serve to promote more rapid neutrophil chemotaxis, which could be contributing to the overall immunopathology.

Interestingly, the adoptive bone marrow transfer experiment did little to negate the effects of the loss of Ifitm3 in *Ifitm3*$^{-/-}$ mice, with a broadly similar phenotype occurring as that seen earlier in the study with non-chimeric mice. This would suggest that possessing immune cells with functioning copies of *Ifitm3* is not sufficient to rescue the *Ifitm3*$^{-/-}$ animal; it would appear as though the altered viral kinetics in the lungs is perhaps the primary cause of the overall phenotype. Further to this, infection with the delNS1 strain of PR/8 influenza virus would also indicate that the phenotype was not the result of impeded IFN production as such attenuated viruses are pathogenic to IFN-deficient mice (Garcia-Sastre *et al.* 1998). Taken cumulatively, these data would suggest the murine phenotype is a result of elevated and sustained viral replication in the respiratory tract and subsequent immune dysregulation; therein causing severe pathological damage.

Since publication of this work (Everitt *et al.* 2012), another group has independently verified our findings by showing the increased susceptibility of mice carrying the *Ifitm3*-null allele (Bailey *et al.* 2012). They also show that heterozygotic *Ifitm3*$^{+/-}$ mice display an intermediate phenotype, and that mice carrying a cumulative deletion of *Ifitm1*, *Ifitm2* and *Ifitm3* are phenotypically

indistinguishable from *Ifitm3*$^{-/-}$ mice; supporting the premise that Ifitm3 is the crucial member of the Ifitm family that controls influenza virus infection *in vivo*.

The prevalence of the rs12252-C SNP in the sampled cohort of hospitalised patients is particularly interesting, as it suggests a heritable trait that can account for viral susceptibility; just as the CCR5-Δ32 mutation can aid resistance to HIV (Dean *et al.* 1996; Samson *et al.* 1996). As discussed previously, the 2009 H1N1 virus was less virulent than was first anticipated; resulting in far fewer mortalities than would be predicted from a novel zoonotic virus. What was remarkable was the prevalence of severe illness and death in individuals that had no known co-morbidities that were not classed as traditionally "at risk" (Donaldson *et al.* 2009). The discovery of the increased susceptibility of the rs12252-CC containing cells and loss of restrictive capacity of NΔ21 IFITM3-expressing cells suggests an important role for fully functional IFITM3 in humans. It is the elucidation of host resistance and susceptibility factors, such as the rs12252-C SNP in IFITM3 that may aid in prediction of disease severity. Although there are clearly many more host factors that may be contributing to the overall illness stemming from influenza virus, our findings provide the first evidence of such a phenomenon.

Recently, these findings have been independently verified in a Chinese cohort of patients, where the prevalence of the rs12252-C SNP is far higher than in European Caucasian populations (Zhang *et al.* 2013b). The study found a significant overrepresentation of the minority SNP in patients hospitalised with severe influenza infection, as well as higher viral loads and levels of MCP-1 in these patients, which are features recorded in our study's *in vivo* murine work (Figures 4.8 and 4.19a). Although the rs12252-CC genotype is rare in Europeans (0.5%), it is far more frequent in Chinese (25%) and Japanese (44%) populations. This data therefore highlights the importance of the SNP, as potentially large numbers of people could possess this genotype; therefore making them more susceptible to the range of viruses that IFITM3 can restrict.

Taken together, this study shows how the loss of a single immune effector, Ifitm3, can transform a potentially mild influenza virus infection into one with remarkable severity. The enrichment of the rs12252 C-allele in those hospitalised with influenza infections, together with the decreased IFITM3 levels and the increased infection of the rs12252-CC cells *in vitro*, suggests that IFITM3

also plays a pivotal role in defence against human influenza virus infections. This innate resistance factor is all the more important during encounters with a novel pandemic virus, when host acquired immune defences are less effective. Indeed, IFITM3-compromised individuals, and in turn populations with a higher percentage of such individuals, may be more vulnerable to the initial establishment and spread of a virus against which they lack adaptive immunity, which would suggest novel vaccination practices should be evaluated to include such groups. In light of its ability to curtail the replication of a broad range of pathogenic viruses *in vitro*, these *in vivo* results suggest that IFITM3 may also shape the clinical course of additional viral infections in favour of the host.